High-resolution calorimetric study of a liquid crystalline organo-siloxane tetrapode with a biaxial nematic phase

George Cordoyiannis,[1] Daniela Apreutesei,[2] Georg H. Mehl,[2] Christ Glorieux,[1] and Jan Thoen[1,*]

[1]*Laboratorium voor Akoestiek en Thermische Fysica, Departement Natuurkunde en Sterrenkunde,*
Katholieke Universiteit Leuven, Celestijnenlaan 200D, B-3001 Leuven, Belgium
[2]*Department of Chemistry, The University of Hull, Cottigham Road, Hull HU6 7RX, United Kingdom*

High-resolution adiabatic scanning calorimetry and differential scanning calorimetry have been employed to study the thermal behavior of an organo-siloxane tetrapode reported to exhibit a biaxial nematic phase. No signature of the uniaxial to biaxial nematic phase transition could be retraced in sequential heating and cooling runs under different scanning rates, within the experimental resolution. The results obtained reveal that an extremely small heat should be involved in the uniaxial to biaxial nematic phase transition. The isotropic to uniaxial nematic transition at 318 ± 0.01 K is very stable, and it is weakly first order with a rather small latent heat of 0.20 ± 0.02 J/g.

PACS number(s): 64.70.M−, 07.20.Fw

I. INTRODUCTION

The existence of the biaxial nematic phase was theoretically predicted in 1970 by Freiser [1] in terms of a generalized Maier-Saupe theory. Theoretical phase diagrams were proposed right after by Alben [2] and Straley [3], and the first experimental proof appeared a few years later for a lyotropic system [4]. On the contrary, in thermotropic systems the situation remained elusive for many years [5]. In the late 1990s, some reports on biaxiality appeared, but only in samples sandwiched between glass plates or in free-standing films [6,7]. It was only in the last five years that new reports on thermotropic biaxiality came out for liquid crystalline polymers [8,9], bow-shaped liquid crystals [10–15], and liquid-crystalline organo-siloxane tetrapodes [16–18].

The first experimental indications of thermotropic biaxiality attracted immediately a significant interest in this field of research [19], also, because of the high potential for applications. The orientation of the secondary director exhibits remarkably improved response times to an applied external field, compared to the ones of the primary director [20,21]. Illatively, the existence of a thermotropic biaxial nematic phase in ambient temperatures is expected to give a new boost to liquid crystal display technology. Simultaneously with the experimental search for thermotropic biaxiality, a great interest was raised for theoretical and simulation studies on systems exhibiting isotropic (I), uniaxial nematic (N_U), and biaxial nematic (N_B) phases [22–32].

Any kind of direct information concerning the type of N_U-N_B phase transition (e.g., first or second order, universality class) has been completely absent from the literature so far. High-resolution calorimetric measurements can shed light on this point and, moreover, they can be employed to explore the fascinating theoretically proposed phase diagrams. In some initial studies these diagrams were considered to have a special kind of critical point, where two lines of second-order transitions merge with a line of first-order ones in a sharp cusp [2,3]. In recent studies, they are expected to include a tricritical point where a line of second-order transitions meets a line of first-order ones and a Landau (triple) point where all three phases I, N_U, and N_B coexist in equilibrium [22,26,30]. Consequently, apart from the great interest for applications, the existence of a thermotropic N_B phase and the study of the N_U-N_B transition are also intriguing from a fundamental point of view.

II. MATERIALS AND METHODS

The compound under investigation is an organo-siloxane tetrapode—namely, compound A in Ref. [16]—and it was synthesized in the Chemistry Department at the University of Hull. Further down we will refer to it as DW-16. Its chemical structure and phase sequence are shown in Fig. 1. Each molecule of DW-16 consists of four (asymmetric) mesogens connected to a siloxane core through spacers. Infrared (IR) absorbance and conoscopic measurements have shown for this tetrapode an I-N_U transition at ∼320 K and an N_U-N_B transition at ∼310 K [16].

In this work, we employed high-resolution adiabatic scanning calorimetry (ASC) and differential scanning calorimetry (DSC) to perform a thorough investigation of the thermal behavior of DW-16. The thermal properties were initially investigated using a Mettler Toledo differential scanning calorimeter (DSC 822^e) in nitrogen against an indium standard. Transition temperatures were determined as the onset of the maximum in the endotherm or exotherm. The ASC measurements were performed in a calorimeter consisting of
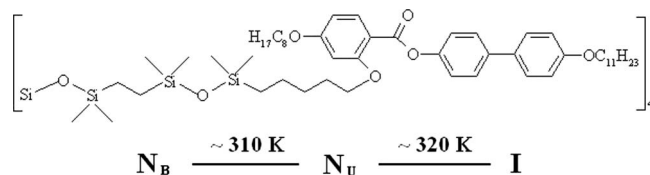

FIG. 1. Molecular structure, phase sequence, and transition temperatures of the DW-16 compound.
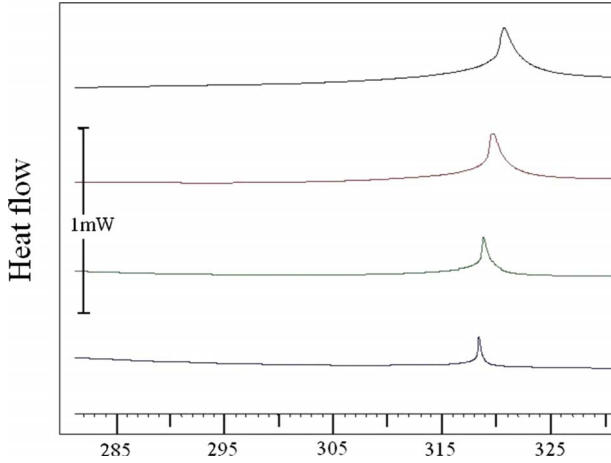
*jan.thoen@fys.kuleuven.be

FIG. 2. (Color online) DSC heating runs of 20, 10, 5, and 2 K/min (from top to bottom). Note that the thermographs have been shifted along the *y* axis.

FIG. 3. (Color online) DSC cooling runs of 2, 5, 10, and 20 K/min (from top to bottom). Note that the thermographs have been shifted along the *y* axis.

four stages. The inner stage is a cylindrical cell, and it is surrounded by three outer shields. The space between the cell and the shields is vacuum pumped in order to achieve excellent thermal insulation between them. ASC yields both the heat capacity (C_p) and enthalpy (H) temperature dependence. It can easily and reliably distinguish between first- and second-order phase transitions and reveals subtle features of $C_p(T)$. A detailed description of our apparatus can be found elsewhere [33,34]. For our measurements we used a 10-g molybdenum cell, which contained 0.237 g of DW-16. In order to eliminate any possible temperature gradients in the sample, a small molybdenum stirring ball was inserted in the cell. Then, by periodically changing the inclination of the whole apparatus (via an automatized mechanism), the stirring ball was moving back and forth inside the cylindrical cell during the experiments. The heat capacity of the empty cell, which was measured in one separate control experiment, was subtracted and the result was divided by the sample mass in order to obtain the net specific heat capacity of the sample.

III. RESULTS AND DISCUSSION

In this section the results for sequential runs using DSC and ASC are reported. The initial thermal investigation was performed by means of DSC using scanning rates between 2 and 20 K/min in the temperature range from 260 to 330 K. The sequential heating and cooling runs revealed the *I*-N_U transition between 315 and 320 K, depending on heating or cooling as well as on the rate used in each run. No peak could be detected in the range of temperatures where the N_U-N_B transition was expected according to previous IR and conoscopic measurements [16]. The DSC results can be seen in Figs. 2 and 3 for heating and cooling runs, respectively.

To perform a more thorough thermal study we employed ASC, using very slow scanning rates (2–3 orders of magnitude slower than the ones of DSC). We carried out a number of sequential heating and cooling runs in the range between room temperature and 325 K. Details of the ASC runs are
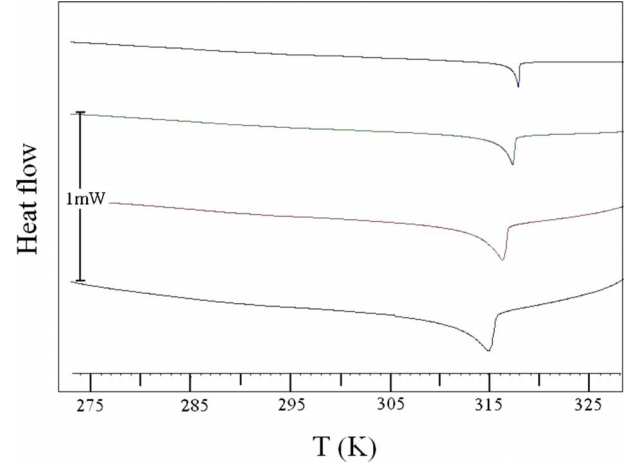
shown in Table I. Concerning the scanning rates, it is noteworthy that they represent average values. In the vicinity of a phase transition the actual rate is slower since the (constant) applied power is spent on both temperature change and conversion between phases. Prior to cooling runs the samples were heated up to the *I* phase and then stabilized to the initial temperature.

In Fig. 4 the $C_p(T)$ curve is shown for the first heating run. The *I*-N_U transition is clearly visible, but no heat capacity anomaly can be detected in temperatures around 310 K, where the N_U-N_B transition is expected according to Ref. [16]. The specific heat capacity and enthalpy temperature dependence in the area around the *I*-N_U phase transition are shown on the top and bottom of Fig. 5, respectively. They are obtained from the second run (see Table I). The insets show the magnified data in a short range of 100 mK around the transition. The *I*-N_U phase transition was always found at the same temperature $T_{I\text{-}N_U} = 318.06 \pm 0.01$ K for the different heating and cooling runs, confirming the high stability of this compound. This transition is very weakly first order with a latent heat $L = 0.20 \pm 0.02$ J/g released over a narrow temperature range of 22 ± 2 mK. This latent heat is remarkably small, compared to the usually measured ones for other liquid crystals [35]. The total transition heat (latent heat plus pretransitional increases) for the *I*-N_U transition obtained by

TABLE I. The features of ASC scans performed for the DW-16 compound.

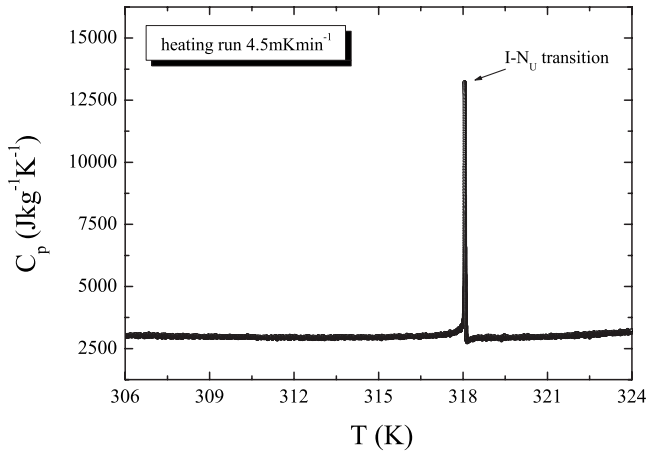| Number of run	Type of run	*T* range (K)	Rate (mK/min)
1	Heating	305.15–325.15	4.5
2	Cooling	325.15–299.15	2.5
3	Cooling	309.15–295.15	2.5
4	Cooling	322.15–295.15	2.5
5	Heating	311.15–323.15	4.5
6	Cooling	313.15–303.15	2.0
7	Heating	295.15–323.15	56.8

FIG. 4. Temperature profile of the specific heat capacity for the first heating run of DW-16. The I-N_U transition occurs at 318.06 K, but there is no visible trace of an N_U-N_B transition.

DSC and ASC are in very good agreement, yielding $\Delta H_{DSC} = 1.3 \pm 0.1$ J/g and $\Delta H_{ASC} = 1.27 \pm 0.05$ J/g, respectively.

A schematic overview of the location of the observed peaks for all ASC runs is presented in Fig. 6. In the temperature range where an N_U-N_B transition was found in Ref. [16],
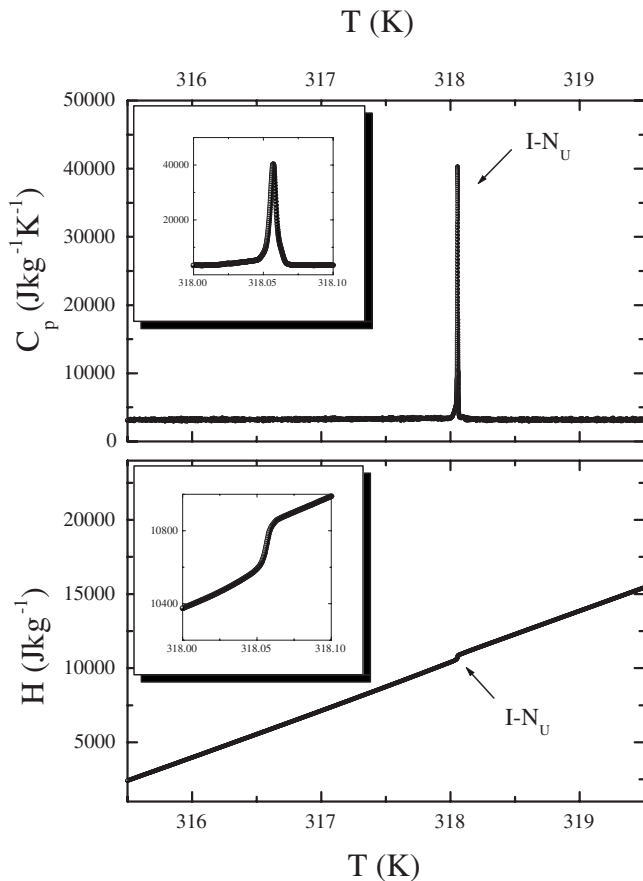

FIG. 5. Heat capacity (top) and enthalpy (bottom) curves for the I-N_U phase transition, with blowups of the 100-mK area around the transition temperature as insets. In the enthalpy curve a linear background is subtracted from the original data for clarity. The data plotted here correspond to the first cooling run (see Table I).
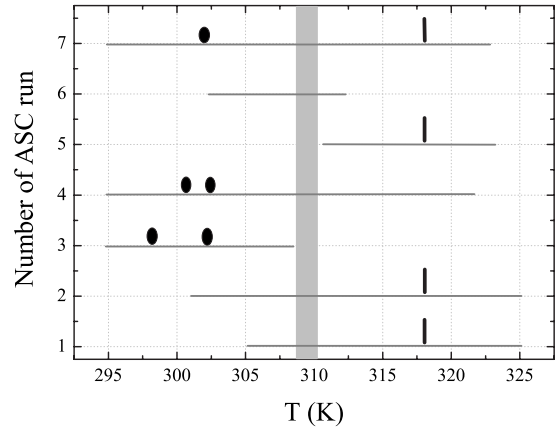

FIG. 6. A schematic overview of the ASC runs and the observed peaks. The spikes correspond to the I-N_U transition temperature and the ellipsoidal symbols to the solidification and melting of DW-16. The shady area, in light-gray color, represents the temperature range where a signature of the N_U-N_B transition was expected according to Ref. [16].

no specific heat capacity anomaly is observed in any of the runs here, as shown in Fig. 7. The maximum C_p noise in slow scans never exceeded the $\pm 1\%$ of the absolute values and, therefore, it cannot be attributed to any kind of phase transition. The absence of an N_U-N_B peak means that this transition must involve an extremely small enthalpy change, smaller than the experimental accuracy of 1 mJ/g for our measurements.

Between the various runs of Fig. 7 one may observe small differences in the slope of $C_p(T)$ curves. They occur because of the approach toward vicinal phase transitions—namely, the I-N_U transition in higher temperatures and the solidification of the sample in lower temperatures (for this transition see the text later on). The data were collected upon heating or cooling and with different scanning rates, as can be identified from Table I. As a consequence, the transition tempera-
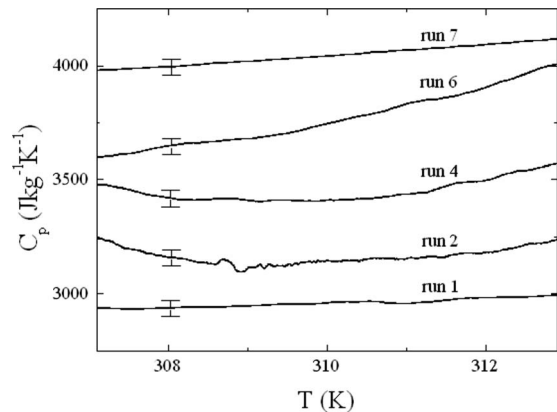

FIG. 7. A detailed plot of specific heat capacity in the temperature range between 307 and 313 K, where a trace of the N_U-N_B transition is expected. The different data sets have been shifted along the y axis for clarity. For each case, the number of run corresponds to the number written in Table I. The changes of C_p values are negligible, as can be seen in comparison with the artificially added error bars of $\pm 1\%$.
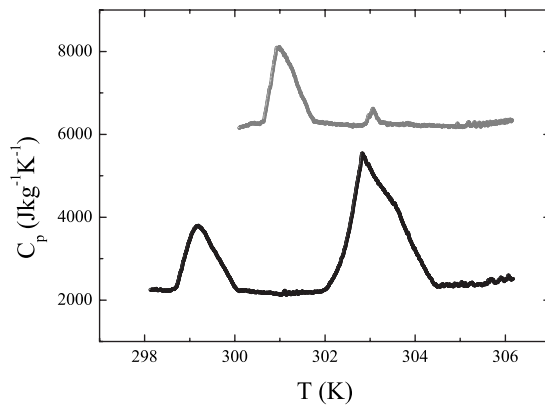
FIG. 8. The specific heat capacity profiles in low temperatures for the second (black symbols) and third (gray symbols) cooling runs (third and fourth runs in Table I, respectively), showing the first-order solidification-melting transitions of DW-16. The latter curve (third cooling run) has been shifted along the y axis for clarity.

tures and/or the pretransitional effects can be sufficiently affected, resulting in slight changes of the $C_p(T)$ background further away from transition temperatures. Dissimilarities in the shape (e.g., sharpness and pretransitional wings) of C_p anomalies are observable even among different very slow runs, as comes out from a comparison of the stable I-N_U peak between heating of Fig. 4 and cooling of Fig. 5.

Below 305 K and close to room temperature strongly first-order transitions have been observed on both heating and cooling runs. These transitions were very dependent on the scanning rate and the thermal history of the sample, and they are attributed to the solidification (upon cooling) and melting (upon heating) of the sample. As can be seen in Fig. 8, in the case of slow cooling runs two separate but still relatively wide strongly first-order anomalies are observed.

Upon the last fast (in terms of ASC) heating run (see Table I) these two peaks are again observed, but unified as a significantly broadened C_p anomaly, which cannot be easily distinguished if plotted on the same scale as the slow cooling runs of Fig. 8. The reason why these transitions are not observed in some of the DSC runs at similar temperatures is possibly caused by supercooling, due to the very fast rates, and subsequent heating of the sample.

IV. SUMMARY

We have studied experimentally the phase transitions of an organo-siloxane tetrapode, which was reported to exhibit an N_B phase [16]. In sequential heating and cooling runs, and within a range of very fast (DSC measurements) down to very slow (ASC measurements) scanning rates, the N_U-N_B phase transition was not discernible. From our measurements it is concluded that a very small transition heat must be related to the N_U-N_B transition, which for DW-16 should be less than 1 mJ/g. This observation is in accordance with previous measurements for a bent-core mesogen, where the transition flaunting under x rays did not leave any thermal trace in DSC thermographs [14]. On the other hand, the I-N_U transition was very stable and weakly first order with a rather small latent heat of 0.20 ± 0.02 J/g compared to other compounds [35].

[1] M. J. Freiser, Phys. Rev. Lett. **24**, 1041 (1970).

[2] R. Alben, Phys. Rev. Lett. **30**, 778 (1973).

[3] J. P. Straley, Phys. Rev. A **10**, 1881 (1974).

[4] L. J. Yu and A. Saupe, Phys. Rev. Lett. **45**, 1000 (1980).

[5] G. R. Luckhurst, Thin Solid Films **393**, 40 (2001).

[6] S. Chandrasekhar, G. G. Nair, K. Praefcke, and D. Singer, Mol. Cryst. Liq. Cryst. Sci. Technol., Sect. A **288**, 7 (1996).

[7] S. Chandrasekhar, G. G. Nair, D. S. Shankar Rao, and S. Krishna Prasad, Liq. Cryst. **24**, 67 (1998).

[8] K. Severing and K. Saalwachter, Phys. Rev. Lett. **92**, 125501 (2004).

[9] K. Severing, E. Stibal-Fischer, A. Hasenhindl, H. Finkelmann, and K. Saalwachter, J. Phys. Chem. B **110**, 15680 (2006).

[10] B. R. Acharya, A. Primak, T. J. Digenmans, E. T. Samulski, and S. Kumar, Pramana, J. Phys. **61**, 231 (2003).

[11] L. A. Madsen, T. J. Dingemans, M. Nakata, and E. T. Samulski, Phys. Rev. Lett. **92**, 145505 (2004).

[12] B. R. Acharya, A. Primak, and S. Kumar, Phys. Rev. Lett. **92**, 145506 (2004).

[13] C. V. Yelamaggad, S. Krishna Prasad, G. G. Nair, I. S. Shash-ikala, D. S. Shankar Rao, G. V. Lobo, and S. Chandrasekhar, Angew. Chem., Int. Ed. **43**, 3429 (2004).

[14] V. Prasad, S. W. Kang, K. A. Suresh, L. Joshi, Q. Wang, and S. Kumar, J. Am. Chem. Soc. **127**, 17224 (2005).

[15] S. Krishna Prasad, G. G. Nair, D. S. Shankar Rao, G. V. Lobo, I. Shashikala, and C. V. Yelemaggad, Mol. Cryst. Liq. Cryst. **437**, 211 (2005).

[16] K. Merkel, A. Kocot, J. K. Vij, R. Korlacki, G. H. Mehl, and T. Meyer, Phys. Rev. Lett. **93**, 237801 (2004).

[17] J. L. Figueirinhas, C. Cruz, D. Filip, G. Feio, A. C. Ribeiro, Y. Frere, T. Meyer, and G. H. Mehl, Phys. Rev. Lett. **94**, 107802 (2005).

[18] K. Neupane, S. W. Kang, S. Sharma, D. Carney, T. Meyer, G. H. Mehl, D. W. Allender, S. Kumar, and S. Sprunt, Phys. Rev. Lett. **97**, 207802 (2006).

[19] G. R. Luckhurst, Nature (London) **430**, 413 (2004).

[20] J. H. Lee, T. K. Lim, W. T. Kim, and J. I. Jin, J. Appl. Phys. **101**, 034105 (2007).

[21] R. Berardi, L. Muccioli, and C. Zannoni, J. Chem. Phys. **128**, 024905 (2008).

[22] A. M. Sonnet, E. G. Virga, and G. E. Durand, Phys. Rev. E **67**, 061701 (2003).

[23] B. Mettout, Phys. Rev. E **72**, 031706 (2005).

[24] M. A. Bates and G. R. Luckhurst, Phys. Rev. E **72**, 051702 (2005).

[25] L. Longa, P. Grzybowski, S. Romano, and E. Virga, Phys. Rev. E **71**, 051714 (2005).

[26] G. De Matteis and E. G. Virga, Phys. Rev. E **71**, 061703 (2005).

[27] G. De Matteis, S. Romano, and E. G. Virga, Phys. Rev. E **72**, 041706 (2005).

[28] F. Bisi, E. G. Virga, E. C. Gartland, Jr., G. De Matteis, A. M. Sonnet, and G. E. Durand, Phys. Rev. E **73**, 051709 (2006).

[29] J. Peláez and M. R. Wilson, Phys. Rev. Lett. **97**, 267801 (2006).

[30] F. Bisi, S. Romano, and E. G. Virga, Phys. Rev. E **75**, 041705 (2007).

[31] L. Longa, G. Pajak, and T. Wydro, Phys. Rev. E **76**, 011703 (2007).

[32] A. G. Vanakaras and D. J. Photinos, J. Chem. Phys. **128**, 124512 (2008).

[33] J. Thoen, H. Marynissen, and W. Van Dael, Phys. Rev. A **26**, 2886 (1982).

[34] J. Thoen, Int. J. Mod. Phys. B **9**, 2157 (1995).

[35] B. Van Roie, J. Leys, K. Denolf, C. Glorieux, G. Pitsi, and J. Thoen, Phys. Rev. E **72**, 041702 (2005).